BIOCHEMISTRY
including biophysical chemistry & molecular biology
Article

*Biochemistry* **2009,** *48,* 10437–10445 10437
DOI: 10.1021/bi901318a

# Flip-Flop Is the Rate-Limiting Step for Transport of Free Fatty Acids across Lipid Vesicle Membranes†

Andrew N. Carley and Alan M. Kleinfeld*

*Torrey Pines Institute for Molecular Studies, 3550 General Atomics Court, San Diego, California 92121*

*Received July 29, 2009; Revised Manuscript Received September 22, 2009*

ABSTRACT: The mechanism of transport of free fatty acids (FFA) across lipid bilayer membranes remains a subject of debate. The debate is whether the rate-limiting step for transport is flip-flop across the membrane or dissociation into the aqueous phase. Recently, a new method for assessing dissociation was described in which fluorescein phosphatidylethanolamine (FPE) introduced into the outer leaflet of lipid vesicles was used to monitor FFA dissociation. Transport of FFA into vesicles containing both FPE in the outer leaflet and pyranine trapped in the inside aqueous phase revealed identical rate constants for quenching of FPE and pyranine fluorescence. Because no difference was observed in the time for FFA binding to the outer surface and flip-flop across the bilayer, it was concluded that dissociation was slower than flip-flop. Here, we used FPE and BSA to assess dissociation of oleate from lipid vesicles. In separate pyranine- or ADIFAB-containing vesicles, we assessed flip-flop. We found that the FPE and BSA transfer methods yielded equivalent rate constants for dissociation, which were 3−10-fold faster than that of flip-flop. We found that in vesicles containing both FPE and pyranine, pyranine fluorescence cannot be separated from FPE fluorescence. The identical rate constants for FPE and pyranine observed with vesicles containing both fluorophores reflected the dominance (20-fold) of FPE fluorescence at pyranine excitation and emission wavelengths. Because the dissociation rate constants are 3−10 times faster than the rate constants for flip-flop, flip-flop must be the rate-limiting step for the transport of FFA across lipid vesicles.

Circulating free fatty acids (FFA)[1] play a central role in physiologic homeostasis. FFA are a major source of energy, are components of more complex molecules, and are mediators of cell signaling. Maintenance of these functions requires regulation of circulating FFA levels, which in turn depends upon the rates of transport of FFA into and out of the cells that store and metabolize FFA. There is considerable interest in the mechanism of membrane transport of FFA because of the possibility that transport might be regulated at the level of the cell membrane. The central issue, for which there is currently no consensus, is whether FFA translocation occurs as rapid diffusion through the lipid phase or whether it requires facilitation by membrane proteins (*1*−*3*). Evidence of extremely rapid diffusion through the lipid phase of membranes is supported by studies reporting that transport of FFA across pure lipid membranes is limited by the rate of dissociation from the lipid bilayer rather than flip-flop, the rate of crossing from one hemileaflet to the other (*1*, *4*−*8*). In contrast, our laboratory has reported that flip-flop is rate-limiting and has activation thermodynamic characteristics distinctly different from those of dissociation (*9*−*13*).

Whether flip-flop or dissociation is rate-limiting for transport of long chain FFA across lipid bilayer vesicles was reexamined recently using a new method to detect the presence of FFA in the outer hemileaflet of lipid vesicles (*14*). In that study, the change in fluorescence of fluorescein-labeled phosphatidylethanolamine (FPE) was used to detect the presence of FFA in the outer leaflet of lipid vesicles. FPE fluorescence was quenched upon binding of FFA to the vesicles, and conversely, FPE fluorescence increased upon dissociation of FFA from the outer leaflet. Dissociation and flip-flop were monitored in small (SUV) and large (LUV) unilamellar vesicles prepared with pyranine trapped in the inside aqueous phase and with FPE present in the outer leaflet of these vesicles (*14*). Movement of FFA from the outer leaflet to the inner leaflet of the vesicles results in quenching of the fluorescence of the trapped pyranine. Conversely, dequenching of the pyranine fluorescence occurs as FFA move from the inner to outer leaflet as described previously (*6*, *7*, *12*).

Using these FPE/pyranine vesicles as acceptor vesicles, Simard et al. (*14*) assessed the transfer of FFA from donor (nonfluorescent) vesicles by monitoring the time courses of the quenching of FPE and pyranine fluorescence. The results for SUV revealed identical rate constants of 7.2 $s^{-1}$ for oleate (OA) quenching of both FPE in the outer leaflet and pyranine inside the SUV. This suggests that there is virtually no lag in time between binding of OA to the outer leaflet and flip-flop of OA from the outer to inner leaflet and would indicate that the rate constant for flip-flop is much faster than 7.2 $s^{-1}$. These results would seem to provide strong support for dissociation of OA from the donor vesicles, rather than flip-flop, being the rate-limiting step for transport of FFA across lipid vesicles.

To resolve the discrepancy with our previous results, we conducted studies similar to those of Simard et al. (*14*) by

†This work was supported by Grant DK058762 from the National Institute of Diabetes and Digestive and Kidney Diseases of the National Institutes of Health. A.N.C. is supported by an American Heart Association Postdoctoral Fellowship.

*To whom correspondence should be addressed: Torrey Pines Institute for Molecular Studies, 3550 General Atomics Ct., San Diego, CA 92121. Telephone: (858) 455-3724. Fax: (858) 455-3792. E-mail: akleinfeld@tpims.org.

[1]Abbreviations: FABP, fatty acid binding protein; rI-FABP, rat intestinal FABP; ADIFAB, acrylodan-labeled rI-FABP; BSA, bovine serum albumin; EPC, egg phosphatidylcholine; FFA, free fatty acids; $FFA_u$, unbound FFA; FPE, fluorescein phosphatidylethanolamine; LUV, large unilamellar vesicles; OA, oleic acid (18:1 Δ9); SUV, small unilamellar vesicles.

© 2009 American Chemical Society
Published on Web 09/24/2009

investigating FFA transport using FPE-labeled and pyranine-containing lipid vesicles. We find, in agreement with Simard et al. (*14*), that monitoring FPE fluorescence provides an accurate measure of the dissociation rate of FFA. However, we demonstrated that pyranine fluorescence cannot be separated from FPE fluorescence in vesicles containing both fluorophores. In contrast to those of Simard et al., our results, using separate FPE- and pyranine-containing lipid vesicles to assess dissociation and flip-flop, respectively, demonstrate that flip-flop is rate-limiting and ~3−10-fold slower than dissociation.

## EXPERIMENTAL PROCEDURES

*Materials*. Egg phosphatidylcholine (EPC) was purchased from Avanti Polar Lipids, Inc. (Alabaster, AL). Sodium salts of oleate (OA) were purchased from NuChek Prep (Elysian, MN), and stock solutions were prepared in water containing 4 mM NaOH (pH 11) and 50 $\mu$M butylated hydroxytoluene. Fluorescein-labeled dihexadecanoylphosphoethanolamine (FPE) and pyranine (8-hydroxypyrene-1,3,6-trisulfonic acid) were purchased from Invitrogen. Acrylodan-labeled rat intestinal fatty acid binding protein (ADIFAB) was prepared as described previously (*15*) and is available from FFA Sciences LLC (San Diego, CA). Fatty acid free BSA was purchased from Sigma-Aldrich (St. Louis, MO). The buffer used in FFA transport experiments contained 20 mM Hepes, 140 mM NaCl, and 5 mM KCl (pH 7.4) (buffer A), and both the OA−BSA complexes and the vesicles were prepared in this buffer.

*Vesicle Preparation*. Vesicles composed of EPC were prepared as described previously (*12*). Small unilamellar vesicles (SUV) were prepared by sonication in buffer A in the presence or absence of 0.1 and 2 mM pyranine. Large unilamellar vesicles (LUV) were prepared by extrusion also in buffer A, with or without 2 mM trapped pyranine or 400 $\mu$M ADIFAB. We prepared FPE vesicles by incubating them at 22 °C with 1 mol % FPE for 1 h while rocking them as described by Simard et al. (*14*). Vesicles were chromatographed through Sephacryl S-1000 to separate free and trapped pyranine and unincorporated FPE. Free ADIFAB was removed by dialysis. The vesicle phospholipid concentration was determined from total inorganic phosphate as described previously (*12*). Vesicle concentrations used in the stopped-flow experiments were 50 $\mu$M. All stopped-flow concentrations refer to values in the mixing chamber, not in the syringe.

*OA−BSA Complexes and Buffering of Unbound FFA*. Complexes of OA and BSA (OA−BSA) were prepared so that unbound OA ($OA_u$) concentrations were buffered at defined values as described previously (*12*). We prepared OA−BSA complexes by mixing aliquots of NaOA, from a 50 mM stock solution in water with 4 mM NaOH, at 37 °C, with a 600 $\mu$M BSA solution in buffer A, also at 37 °C. The concentration of unbound OA ($[OA_u]$) was monitored using ADIFAB (*16*). For all influx measurements, $[OA_u]$ was 49 nM and [BSA] was 12.5 $\mu$M, in the stopped-flow mixing chamber. The OA−BSA complex at 49 nM $OA_u$ was prepared using an OA:BSA ratio of approximately 3.5:1. For transfer experiments, the donor vesicles were loaded with OA between 2 and 10 mol % EPC. Vesicles were loaded with OA via addition of aliquots of OA from a 0.5 mM OA/4 mM NaOH stock to vesicles stirred at 37 °C. The acceptor BSA concentration was between 2.5 and 5 $\mu$M.

*Fluorescence*. Steady state fluorescence measurements were performed using a Spex Fluorolog-3 fluorometer (JY Horiba). ADIFAB fluorescence was excited at 386 nm, and emission was measured at 432 and 505 nm. Excitation and emission spectra for FPE and pyranine were recorded with excitation and emission slits set at 3 nm. The kinetics of FFA movement were monitored by stopped-flow mixing using a SF-2004 Kintek Instrument (State College, PA) with a resolution of $< 2$ ms in which equal volumes of 0.04 mL reactants were mixed at flow rates of 8 mL/s as described previously (*12*). All concentrations refer to the value in the temperature-controlled mixing chamber. Tryptophan, ADIFAB, pyranine, and FPE fluorescence intensities were monitored by excitation at 290, 386, 455, and 490 nm, respectively, and observation of emission through 20 nm bandwidth filters at 343, 435, 505, and 523 nm, respectively.

Changes in fluorescence intensities of each of the four fluorophores, tryptophan, ADIFAB, pyranine, and FPE, were used to monitor the transfer of OA between different aqueous and vesicle bilayer phases. Quenching of BSA tryptophan fluorescence, caused by binding of OA to BSA, was used to monitor the transfer of OA from vesicles to BSA as described previously (*12*). The change in the fluorescence ratio, upon binding of OA to ADIFAB trapped in the inner aqueous phase of the vesicles, was used to monitor the change in $[OA_u]$ in the inner aqueous phase of the vesicles (*12*). The increase or decrease in fluorescence of FPE-labeled vesicles monitored the decrease or increase, respectively, in the level of OA in the outer hemileaflet of the vesicles, as described by Simard et al. (*14*). The decrease in the fluorescence of pyranine trapped in the inner aqueous phase of the vesicles was used to monitor the decrease in pH as protonated OA flipped from the outer to inner hemileaflet of the vesicles, as described previously (*6*, *12*).

*Kinetic Models of Transport of FFA across Lipid Vesicles*. Differences in the interpretation of experimental observations play a central role in the disagreement concerning the rate-limiting steps in transport of FFA across lipid vesicles. To gain an accurate understanding of the transport steps underlying the measured time courses, a careful analysis of applicable kinetic models of the transport processes is required. We have previously conducted such analyses for several experimental FFA transport studies (*9*−*12*, *17*). Here we describe the models appropriate for transport between donor and acceptor vesicles and between FFA−BSA complexes and vesicles. The models are represented by eqs 1−6 and are illustrated by the reaction schemes in Figure 1.

$$\frac{d[FFA_i]^{D,A}}{dt} = k_{off}[FAm_i]^{D,A} - k_{on}[V][FFA_i]^{D,A} \quad (1)$$

$$\frac{d[FAm_i]^{D,A}}{dt} = k_{ff}([FAm_o]^{D,A} - [FAm_i]^{D,A}) + k_{on}[V][FFA_i]^{D,A} - k_{off}[FAm_i]^{D,A} \quad (2)$$

$$\frac{d[FAm_o]^{D,A}}{dt} = k_{ff}([FAm_i]^{D,A} - [FAm_o]^{D,A}) + k_{on}[V][FFA_o] - k_{off}[FAm_o]^{D,A} \quad (3)$$

$$\frac{d[FFA_o]}{dt} = k_{off}[FAm_o]^{D,A} - k_{on}2[V][FFA_o] \quad (4)$$

$$\frac{d[BSA_b]}{dt} = k_{BSA}^{on}([BSA_T] - [BSA_b])[FFA_o] - k_{BSA}^{off}[BSA_b] \quad (5)$$

$$\frac{d[FFA_o]}{dt} = k_{off}[FAm_o] + k_{BSA}^{off}[BSA_b] - k_{on}[V][FFA_o] - k_{BSA}^{on}([BSA_T] - [BSA_b])[FFA_o] \quad (6)$$

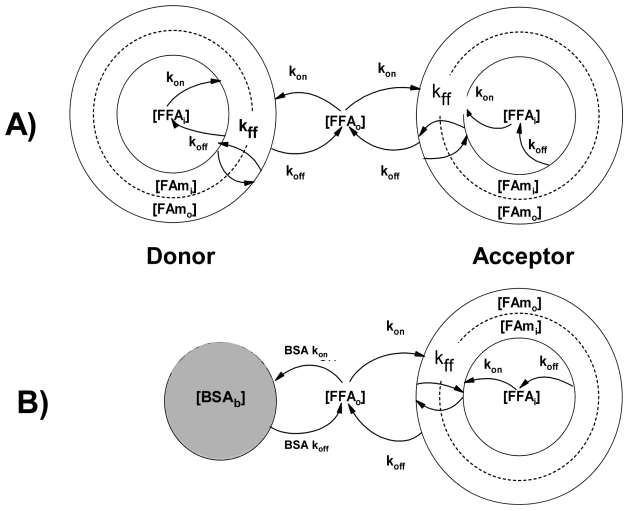


FIGURE 1: Reaction schemes for transport of FFA in lipid vesicles. These models illustrate the distinct FFA compartments and kinetic steps involved in transport of FFA between vesicles and between BSA and vesicles. The concentrations of FFA in the different compartments are as follows: [FFA$_i$], inside aqueous; [FFAm$_i$], inner hemileaflet; [FFAm$_o$], outer hemileaflet; [FFA$_o$], outside aqueous; and [BSA$_b$], bound to BSA. The model rate constants corresponding to the reaction steps are as follows: $k_{on}$, binding from water to vesicle; $k_{off}$, dissociation from vesicle to water; $k_{ff}$, flip-flop between hemileaflets of the vesicle; BSA $k_{on}$, binding from water to BSA; and BSA $k_{off}$, dissociation from BSA to water. (A) Transport of FFA from donor to acceptor vesicles. (B) Transport of FFA from FFA−BSA complexes to acceptor vesicles.

The model appropriate for vesicle to vesicle transport is specified by eqs 1−4 and Figure 1A. The solutions to eqs 1−4 yield the time-dependent FFA concentrations in the internal ([FFA$_i$]) and external ([FFA$_o$]) aqueous phases and in the inner ([FAm$_i$]) and outer ([FAm$_o$]) hemileaflets of the donor and acceptor vesicle bilayers. For the sake of simplicity, we modeled vesicles with equal lipid concentrations ([V]) and therefore equal areas in each hemileaflet of the bilayer. All concentrations are referenced to the total sample volume. The superscripts D,A indicate that there are two sets of eqs 1−4, one each for the donor and acceptor vesicles, respectively. All eight equations must be solved simultaneously to obtain the time dependence of the FFA concentrations in each distinct compartment of Figure 1A. Although we assume, for the sake of simplicity, equal flip-flop rate constants ($k_{ff}$) for inward and outward FFA translocation, the model can be extended to asymmetric flip-flop and vesicle dimensions (SUV), as we described previously (*9*). Solutions were obtained by numerical solution using MLAB (Civilized Software) for specific rate constants, vesicle and FFA concentrations, and initial conditions. Initial conditions were determined from equilibrium conditions, for example, using the partition coefficient $K_p$ to calculate [FAm] and $k_{on}$, as described previously (*11*, *12*, *17*).

The model for transport of FFA between BSA and vesicles is represented by eqs 1−3, 5, and 6, where either acceptor or donor vesicles are used, and the model is illustrated by Figure 1B. Total and bound BSA concentrations are [BSA$_T$] and [BSA$_b$], respectively, and the binding and dissociation rate constants for BSA are denoted with the subscript BSA. We have demonstrated previously that binding of FFA to BSA is described well by six or seven binding sites with equal affinities (*18*) and that $k_{off}$ for BSA is independent of the FFA:BSA ratio (*19*). It follows that $k_{on}$ is also independent of the FFA:BSA ratio. In eqs 5 and 6, [BSA$_T$] and [BSA$_b$] are equivalent to the concentrations of FFA binding sites and bound FFA, respectively.

*Relationship between Model and Observable Rate Constants*. In the experiments performed in this and previous studies, we directly measured the time courses corresponding to [FFA$_i$], from the change in ADIFAB and pyranine fluorescence. We also measured the change in [FAm$_o$], from the change in FPE and BSA fluorescence, and BSA$_b$, from the BSA fluorescence. The rate constants determined from these measured time courses, $k_{in}$, $k_{out}$, and $k_{off}$, may not be equal to model rate constants $k_{ff}$ and $k_{off}$. In general, each of the measured rate constants is a function of both $k_{ff}$ and $k_{off}$. Because there is no general analytic solution to the models of eqs 1−6, we have solved for $k_{ff}$ and $k_{off}$ by using MLAB to numerically fit the models to the measured time courses (*12*) or by comparing experiment to fits of exponential functions to solutions of eqs 1−6.

*Determination of Rate Constants from the Measured Time Courses*. The time course for dissociation of OA from vesicles was monitored (1) by the increase in FPE fluorescence after mixing OA-loaded FPE-labeled SUV with unlabeled acceptor SUV, (2) by the decrease in FPE fluorescence after mixing OA-loaded unlabeled SUV with FPE-labeled acceptor SUV, and (3) by the quenching of BSA tryptophan fluorescence after mixing BSA with OA-loaded SUV or LUV. For SUV, the time courses were monitored over 500 ms and were described well by a single-exponential function whose rate constants were approximately equal to the model dissociation rate constants ($k_{off}$). For LUV, the time course for BSA tryptophan quenching was monitored over 10 s and was fitted well by a two-exponential function, but significantly less well (by $\chi^2$) by a single-exponential function. As discussed previously, the fast component of the two-exponential function is consistent with $k_{off}$ and the slow component with flip-flop (*12*).

Influx rate constants ($k_{in}$) were determined by monitoring the time course of the quenching of pyranine fluorescence after mixing either OA−BSA complexes or donor vesicles loaded with OA with vesicles containing trapped pyranine. For LUV containing ADIFAB, we monitored the influx time course, and determined $k_{in}$, by the increase in the ratio of the ADIFAB emission intensities at 505 nm to 435 nm using OA−BSA complexes to deliver OA. We also used OA-loaded LUV containing ADIFAB to monitor OA efflux, and determined $k_{out}$, as OA transferred from these LUV to fatty acid free BSA. All influx or efflux time courses were fitted well with a single-exponential function from which rate constants $k_{in}$ and $k_{out}$ were determined. For LUV, we also determined $k_{out}$ from the slow component of the BSA tryptophan time course as OA transferred from donor LUV to acceptor BSA.

## RESULTS

*Pyranine Cannot Be Distinguished from FPE Fluorescence in Lipid Vesicles Containing Both Fluorophores*. The conclusion that flip-flop of FFA is faster than dissociation (desorption), in the lipid vesicle study of Simard et al. (*14*), requires that the fluorescence of pyranine and FPE be separable in vesicles containing both fluorophores. In the experiment of Simard et al. (*14*), FPE was incorporated into the outer leaflet of SUV containing trapped pyranine. The transfer of OA from donor SUV to the FPE with pyranine SUV acceptors resulted in the quenching of FPE fluorescence (excitation at 490 nm and emission at 520 nm) and the quenching of pyranine fluorescence (excitation at 455 nm and emission at 509 nm). Both quenching time courses revealed identical rate constants of 7.2 $s^{-1}$ (Figure 2 of ref *14*). This

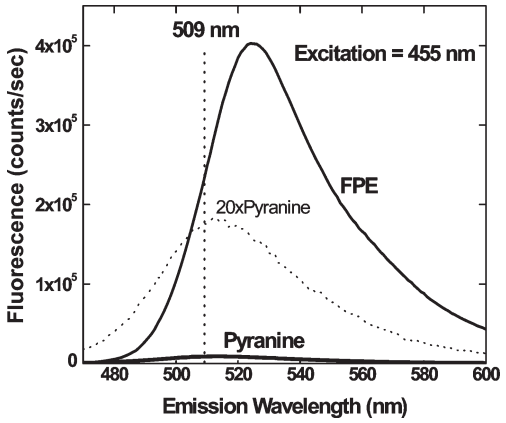


FIGURE 2: Fluorescence intensities from FPE-labeled SUV or from pyranine-containing SUV. (A) SUV were prepared either with 1 mol % FPE or with 0.1 mM pyranine. Emission spectra, obtained using the pyranine excitation wavelength of 455 nm, were collected from both types of SUV with equal EPC concentrations of 25 $\mu$M. The measured spectrum for SUV containing 0.1 mM pyranine is shown as a solid line, and the dotted line is the 0.1 mM spectrum multiplied by a factor of 20 and is virtually identical to the magnitude obtained with vesicles prepared with 2 mM pyranine. SUV labeled with 1% FPE and containing 0.1 mM pyranine were those used in ref *14*.

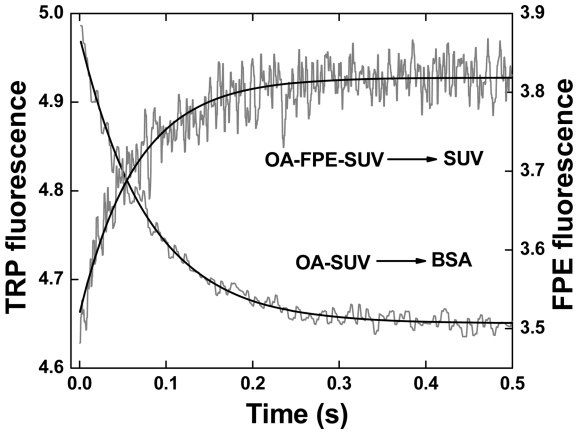


FIGURE 3: Dissociation of OA from SUV. The rate of dissociation of OA from SUV was determined by measuring, at 25 °C, the dequenching of FPE fluorescence as OA transferred from OA-loaded FPE-labeled SUV to SUV acceptors and by measuring the quenching of BSA tryptophan fluorescence as OA transferred from OA-loaded SUV to BSA. The concentration of the SUV was 50 $\mu$M and that of FPE 1 mol %; donor SUV were loaded with 5 $\mu$M OA, and the BSA concentration was 2.5 $\mu$M (all concentrations are in the mixing chamber of the stopped-flow instrument). The time courses (average of more than seven scans) were fitted (solid lines through the data) with single-exponential functions and yielded rate constants of $12.7 \pm 0.2$ s$^{-1}$ for transfer to BSA and $15.2 \pm 0.4$ s$^{-1}$ for transfer from FPE-labeled SUV.

suggested that as soon as FPE detected OA in the outer leaflet of the SUV, pyranine detected OA in the inner leaflet. This finding led to the conclusion that flip-flop was much faster ( $> 69$ s$^{-1}$) than desorption of OA from the donor vesicle (Table 1 of ref *14*).

For this interpretation to be valid, the fluorescence of pyranine and FPE must be distinguishable in vesicles that contain both fluorophores. However, the fluorescence of FPE and pyranine overlaps at the excitation (455 nm) and emission (509 nm) wavelengths used for pyranine (Figure 2). We prepared SUV either with 1 mol % FPE or with 0.1 mM pyranine, the conditions described in ref *14*, and found that the FPE fluorescence was more than 20-fold larger than the pyranine fluorescence at the pyranine wavelengths (Figure 2). The lower pyranine intensity relative to that of FPE is consistent with SUV dimensions (*20*), which predict a pyranine:FPE molar ratio of 0.006 for the SUV of ref *14*. Therefore, the finding of identical rate constants for FPE and pyranine by Simard et al. (*14*) was likely a consequence of the inability to distinguish FPE and pyranine fluorescence in vesicles containing both fluorophores.

*Determination of the Rate Constants for Dissociation of Oleate from Lipid Vesicles*. Simard et al. (*14*) demonstrated how FPE could be used to monitor dissociation of FFA from lipid vesicles. However, the rate constants for dissociation from SUV reported by Simard et al. (*14*) are ~2-fold slower than those reported previously by Massey et al. (*21*) and our laboratory (*12*, *13*). In this study, we used both FPE and a method similar to that of Massey et al. (*21*), as in our previous studies, to determine the rate constants for dissociation of OA from SUV and LUV. To assess dissociation from SUV, we measured the transfer of OA from donor FPE SUV to acceptor SUV, transfer of OA from donor SUV to BSA (Figure 3), and transfer of OA from donor SUV to acceptor FPE SUV (Figure 1S of the Supporting Information). Dissociation of OA from FPE-labeled donor SUV produced an increase in FPE fluorescence; dissociation from donor and transfer to FPE-labeled acceptor SUV quenched FPE fluorescence, and transfer of OA from donor SUV to BSA quenched BSA tryptophan fluorescence. For all three systems, the time courses, at 25 °C, were described well by single-exponential functions, yielding rate constants of $15.7 \pm 1$ s$^{-1}$ for FPE and $12.6 \pm 0.2$ s$^{-1}$ for BSA fluorescence (Table 1). Dissociation of OA from LUV was assessed by measuring transfer from LUV donors to BSA (Figure 4). Quenching of BSA tryptophan was described well by a biexponential function over the 10 s measurement period, with rate constants of $6.2 \pm 0.3$ and $0.6 \pm 0.1$ s$^{-1}$ and similar amplitudes for both components. Tables 1 and 2 summarize the flip-flop and dissociation rate constants for SUV and LUV measured by different methods at 20 and 25 °C, in this study.

Table 1: Rate Constants for OA Transport in SUV[a]

| temp (°C) | $k_{in}$(OA−BSA) | $k_{in}$(SUV donor) | $k_{off}$(FPE) | $k_{off}$(BSA) |
|---|---|---|---|---|
| 20 | $4.2 \pm 0.4$[b] | $4.0 \pm 0.1$ | $12.1 \pm 0.5$ | $11.4 \pm 0.2$ |
| 25 | $6.4 \pm 0.1$ | $4.8 \pm 0.3$ | $15.7 \pm 1.0$ | $12.6 \pm 0.2$ |

[a]Rate constants are in units of s$^{-1}$. Influx rate constants ($k_{in}$) were determined using either OA−BSA complexes [$k_{in}$(OA−BSA)] or OA-loaded donor SUV [$k_{in}$(SUV donor)] to deliver OA to acceptor SUV containing pyranine. Dissociation rate constants ($k_{off}$) were determined using FPE-labeled donor SUV [$k_{off}$(FPE)] and FPE-labeled acceptor SUV or by measuring transfer from donor SUV to BSA [$k_{off}$(BSA)]. [b]Values are averages ± standard deviations of at least three separate measurements, each measurement being an average of at least four separate stopped-flow time courses.

*Influx Rate Constants (flip-flop) for SUV and LUV Are Slower Than Dissociation Constants*. In a previous study, we found that the rate constant for OA influx ($k_{in}$), determined by mixing uncomplexed OA with pyranine-containing vesicles, increased with vesicle concentration (*12*). Because flip-flop is a unimolecular reaction, it cannot depend on vesicle concentration, and therefore, the rate constants measured with uncomplexed FFA cannot be rate constants for flip-flop. In contrast, delivering OA (or other long chain FFA) to vesicles using complexes of FFA with BSA yielded $k_{in}$ values that were independent of vesicle concentration, and therefore, as we argued, such measurements

of $k_{in}$ yielded accurate values for flip-flop rate constants (*12*, *13*). Simard et al., however, argued that the rate constants observed using OA−BSA complexes reflected slow dissociation from BSA rather than flip-flop (Figure 1 of ref *14*), although as we explained in refs *2*, *12*, and *13*, dissociation from BSA is unlikely to be rate-limiting in such measurements.

Because dissociation from SUV is significantly faster [approximately 14 $s^{-1}$ (Table 1)] than from BSA, we have compared OA influx using OA-loaded vesicles and OA−BSA complexes as OA donors to address directly whether slow flip-flop observed with FFA−BSA complexes reflects dissociation from BSA. These measurements of influx of OA into pyranine-containing SUV and LUV were performed, using donor vesicles and the OA−BSA complexes to deliver OA to SUV and LUV. For SUV, we observed similar time courses and influx rate constants for either method of delivery; for OA delivered by an OA−BSA complex for which [$OA_u$] was 49 nM, $k_{in}$ was 6.3 ± 0.1 $s^{-1}$, and for OA delivered by donor SUV loaded with 2 mol % OA, $k_{in}$ was 5.0 ± 0.1 $s^{-1}$ (Figure 5). Similarly for LUV, virtually identical rate constants were observed for either method of OA delivery; $k_{in}$ was 0.63 ± 0.01 $s^{-1}$ for the [$OA_u$] of 49 nM delivered by the OA−BSA complex and 0.60 ± 0.01 $s^{-1}$ delivered by donor LUV loaded with 2 mol % OA (Figure 6). These results demonstrate that (1) $k_{in}$ values measured with OA donated from BSA complexes are similar to those obtained using donor vesicles, (2) using the same OA−BSA complexes yields $k_{in}$ values for SUV that are approximately 10-fold faster than those for LUV, and (3) $k_{in}$ values measured by either method are, at 25 °C, approximately 3 and 10 times slower than those for dissociation from SUV and LUV, respectively. We also determined the (flip-flop) efflux rate constants ($k_{out}$) for LUV from measurements of transfer from donor LUV to BSA (Figure 4). These values (0.6 $s^{-1}$ at 25 °C) are virtually identical to $k_{in}$ and provide additional evidence for slow flip-flop.

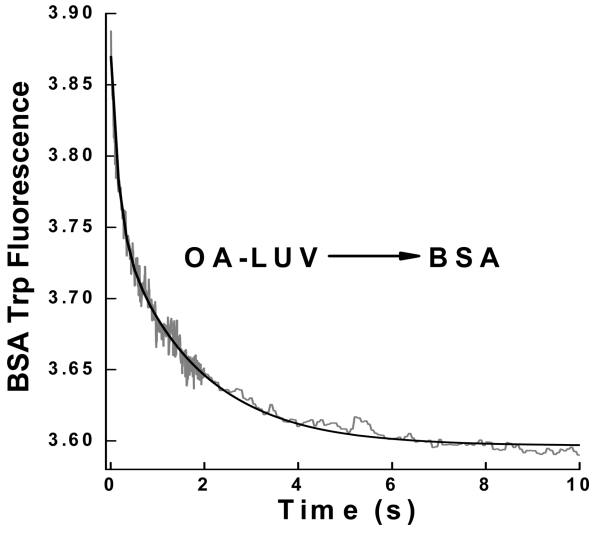


FIGURE 4: Dissociation of OA from LUV. The rate of dissociation of OA from LUV was determined by measuring, at 25 °C, the quenching of BSA tryptophan fluorescence as OA transferred from OA-loaded LUV to BSA. The concentration of the LUV was 50 $\mu$M; the donor LUV were loaded with 5 $\mu$M OA, and the BSA concentration was 2.5 $\mu$M (all concentrations are in the mixing chamber of the stopped-flow instrument). The time courses (average of more than seven scans) were fitted (solid lines through the data) with a two-exponential function (fits with a single-exponential function yielded $\chi^2$ values 3.5-fold larger than for the two-exponential function, and the single fit yielded substantially larger residuals than the double fit) and yielded rate constants of 6.2 ± 0.3 and 0.59 ± 0.13 $s^{-1}$, with similar pre-exponential amplitudes for both components (0.16 and 0.12, respectively).

*LUV Influx and Efflux Rate Constants Monitored with ADIFAB*. Oleate influx rate constants were determined using OA−BSA complexes, for which [$OA_u$] = 49 nM, to deliver OA to LUV containing trapped ADIFAB (Figure 7). The time course of the change in the ADIFAB fluorescence ratio for OA influx yielded a $k_{in}$ rate constant of 0.79 $s^{-1}$. The ADIFAB-trapped LUV were also used to monitor OA efflux by mixing OA-loaded LUV with fatty acid free BSA (Figure 7). The ADIFAB-monitored ratio reveals a time course with a $k_{out}$ rate constant of 0.78 $s^{-1}$. Thus, as we found previously with pyranine-containing vesicles (*12*, *13*), $k_{in} \approx k_{out}$ for LUV. Because efflux does not

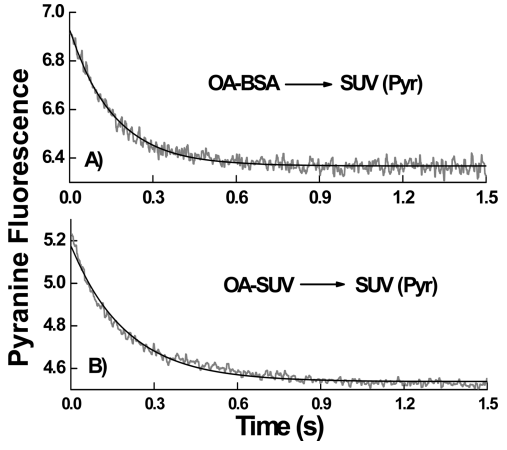


FIGURE 5: OA influx measured with pyranine-containing SUV. Influx of OA into pyranine-containing SUV [2 mM pyranine (Pyr)] was monitored, at 25 °C, using either (A) an OA−BSA complex with an [$OA_u$] of 49 nM (corresponding to [BSA] = 12.5 $\mu$M and [$OA_t$] ~ 50 $\mu$M, within the stopped-flow mixing chamber) as the OA donor and SUV (50 $\mu$M) containing pyranine as the acceptors or (B) 50 $\mu$M SUV loaded with 1 $\mu$M OA as donors to 50 $\mu$M SUV acceptors. Influx rate constants ($k_{in}$) obtained from fitting the stopped-flow time courses (average of more than seven traces) with single-exponential functions were (A) 6.3 ± 0.1 and (B) 5.0 ± 0.1 $s^{-1}$.

Table 2: Rate Constants for OA Transport in LUV[a]

| temp (°C) | $k_{in}$(OA−BSA) | $k_{in}$(LUV donor) | $k_{in}$(ADIFAB) | $k_{out}$(ADIFAB) | $k_{out}$(pyranine) | $k_{off}$(BSA) |
|---|---|---|---|---|---|---|
| 20 | 0.45 ± 0.01[b] | 0.46 ± 0.01 | | | 0.57 ± 0.2 | 5.5 ± 0.2 |
| 25 | 0.63 ± 0.01 | 0.64 ± 0.02 | 0.79 ± 0.01 | 0.80 ± 0.01 | 0.72 ± 0.01 | 6.1 ± 1 |

[a]Rate constants are in units of $s^{-1}$. Influx rate constants ($k_{in}$) were determined using either OA−BSA complexes [$k_{in}$(OA−BSA)] or OA-loaded donor LUV [$k_{in}$(LUV donor)] to deliver OA to acceptor LUV containing pyranine or OA−BSA complexes to deliver OA to ADIFAB-containing LUV [$k_{in}$(ADIFAB)]. Efflux rate constants ($k_{out}$) were determined by measuring transfer to BSA from either donor LUV containing ADIFAB [$k_{out}$(ADIFAB)] or pyrainine [$k_{out}$(pyranine)]. Dissociation rate constants ($k_{off}$) were determined by measuring transfer from donor LUV to BSA [$k_{off}$(BSA)]. [b]Values are averages ± standard deviations of at least three separate measurements, each measurement being an average of at least four separate stopped-flow time courses.

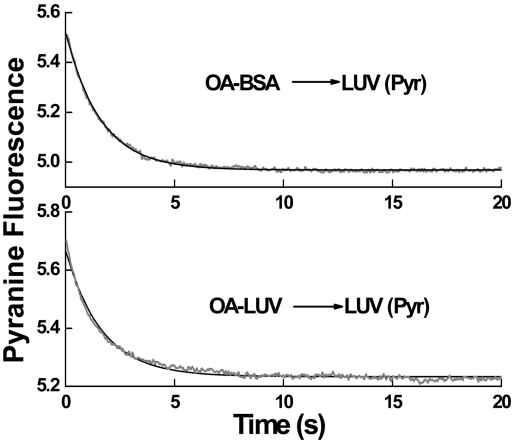


FIGURE 6: OA influx measured with pyranine-containing LUV. Influx of OA into pyranine-containing LUV [2 mM pyranine (Pyr)] was monitored, at 25 °C, using either (A) an OA−BSA complex with an $[OA_u]$ of 49 nM (corresponding to [BSA] = 12.5 $\mu$M and $[OA_t] \sim$ 50 $\mu$M, within the stopped-flow mixing chamber) as the OA donor and LUV (50 $\mu$M) containing pyranine as the acceptors or (B) 50 $\mu$M LUV loaded with 1 $\mu$M OA as donors to 50 $\mu$M LUV acceptors. Influx rate constants ($k_{in}$) obtained from fitting the stopped-flow time courses (average of more than seven traces) with single-exponential functions were (A) 0.63 ± 0.01 and (B) 0.60 ± 0.01 $s^{-1}$.

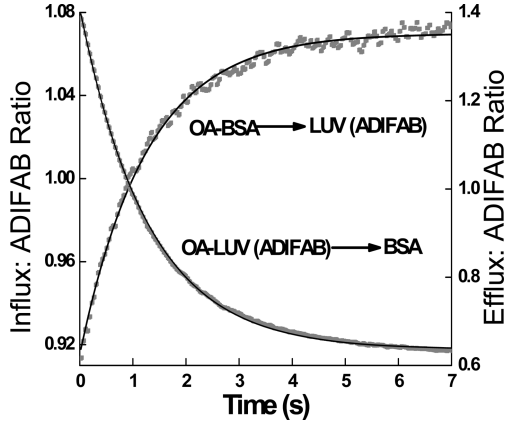


FIGURE 7: Oleate influx and efflux measured in ADIFAB-containing LUV. Influx of OA into ADIFAB-containing LUV was monitored by the increase in the ratio of the 505 nm to 435 nm ADIFAB fluorescence, at 25 °C, using an OA−BSA complex with an $[OA_u]$ of 49 nM (corresponding to [BSA] = 12.5 $\mu$M and $[OA_t] \sim 50$ $\mu$M, within the stopped-flow mixing chamber) as the OA donor and LUV (50 $\mu$M) containing ADIFAB (400 $\mu$M ADIFAB) as the acceptor. Efflux of OA from the ADIFAB-containing LUV (50 $\mu$M), loaded with 1 $\mu$M OA, was monitored by the decrease in the ratio of ADIFAB fluorescence as OA transferred to BSA (2.5 $\mu$M within the stopped-flow mixing chamber) donors to 50 $\mu$M LUV acceptors. Influx ($k_{in}$) and efflux ($k_{out}$) rate constants were obtained from fitting the stopped-flow time courses (average of more than seven traces) with single-exponential functions and yielded values of 0.79 ± 0.02 and 0.78 ± 0.01 $s^{-1}$ for $k_{in}$ and $k_{out}$, respectively.

involve dissociation from BSA and because $k_{in}$ and $k_{out}$ are virtually identical, these results indicate that influx measured with FFA−BSA complexes is independent of dissociation from BSA. Moreover, $k_{in}$ values measured with pyranine and ADIFAB yield similar rate constants, 0.6 and 0.8 $s^{-1}$, respectively (Table 2 and Figures 6 and 7). This provides additional evidence that the rate of dissociation must be faster than $k_{in}$ because detection of OA, by ADIFAB trapped inside the LUV, requires dissociation of OA from the inside bilayer leaflet before binding to ADIFAB.

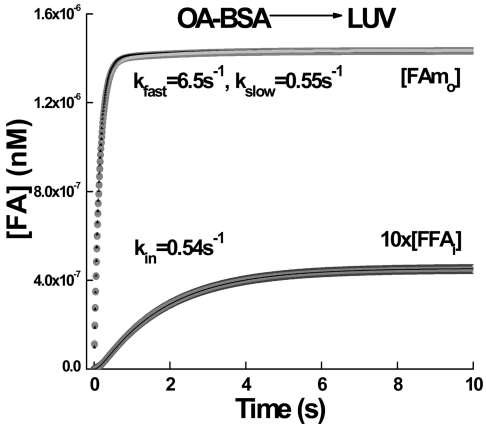


FIGURE 8: Transfer from FFA−BSA complexes to vesicles is independent of the rate constant for dissociation of FFA from BSA. Time courses for transport of FFA from OA−BSA complexes to LUV acceptors were calculated using the kinetic model defined by eqs 1−3, 5, and 6). Results are shown for filling the outer hemileaflet ($[FAm_o]$) and transport into the inside aqueous compartment ($10\times[FFA_i]$), for BSA dissociation rate constants (BSA $k_{off}$) between 0.11 and 11.0 $s^{-1}$ which are 10 times smaller and larger, respectively, than the measured value of 1.1 $s^{-1}$ at 22 °C. As is apparent, the time courses for this 100-fold difference in BSA $k_{off}$ values are virtually identical. Also shown are the rate constants obtained by fits of single-exponential ($[FFA_i]$) and double-exponential ($FAm_o$]) functions to these time courses, which correspond to the measured rate constants for $k_{in}$, and $k_{off}$ plus $k_{out}$, respectively. The following parameters were used for these calculations: [LUV] = 100 $\mu$M, $[BSA_T]$ = 50 $\mu$M (350 $\mu$M OA binding sites), $k_{ff}$ = 0.6 $s^{-1}$, $k_{off}$ = 6.0 $s^{-1}$, $K_p = 4 \times 10^5$, and $K_d$(BSA) = 6 nM [single class of seven sites (*18*)]. The initial conditions were as follows: $[BSA_b(0)]$ = 313 $\mu$M, $[FFA_o(0)]$ = 50 nM, and $[FFAm_o(0)] = [FFAm_i(0)] = [FFA_i(0)] = 0$.

*Kinetic Modeling Provides Important Constraints for the Accurate Interpretation of Measurements of FFA Transport*. Simard et al. (*14*) measured transfer of OA from OA−BSA complexes to pyranine-containing vesicles and interpreted the observed slow rate of quenching of pyranine as being due to the slow dissociation of OA from BSA (BSA $k_{off}$ in Figure 1B) rather than slow flip-flop. We assessed the validity of this interpretation by using the kinetic model (eqs 1−5) to calculate time courses for transfer of FFA from FFA−BSA complexes to vesicles (Figure 8). The results indicated that binding to the outer ($FAm_o$) and inner ($FAm_i$, not shown) hemileaflets and FFA transported into the inside aqueous volume ($FFA_i$) of the vesicles are independent of the rate constant for dissociation from BSA, for $k_{off}$(BSA) values that range from 10-fold less to 10-fold larger than the measured rate constant of 1.1 $s^{-1}$ for BSA (*19*). As we demonstrated previously, for FFA−BSA complexes that buffer $[FFA_u]$ (as in the present case), binding of FFA to vesicles is limited by the vesicle, not the BSA dissociation rate constant (*12*). Thus, contrary to the interpretation of Simard et al. (*14*), their measurements demonstrated slow flip-flop rather than slow dissociation from BSA.

The kinetic model (eqs 1−6) was also used to compare time courses predicted for slow and fast flip-flop for transport of FFA between donor and acceptor vesicles (Figure 2SA of the Supporting Information). The simulations revealed that for slow flip-flop ($k_{ff}$ = 0.6 $s^{-1}$) and rapid dissociation ($k_{off}$ = 6 $s^{-1}$), the time course in the outer hemileaflet ($FAm_o$) was described well by a two-exponential function with rate constants of 6.7 and 0.53 $s^{-1}$. Time courses for the $FAm_i$ and $FFA_i$ compartments of the vesicle were both described well by a single exponential with a rate constant of 0.51 $s^{-1}$. In contrast, vesicles in which transport is

governed by fast flip-flop ($k_{ff}$ = 6 or 20 $s^{-1}$) and slow dissociation ($k_{off}$ = 0.6 or 6 $s^{-1}$) reveal the same single-exponential rate constants of 0.29 and 2.7 $s^{-1}$, respectively, in all three of the vesicle's compartments (Figure 2SB,C of the Supporting Information). As discussed previously, the model predicts that in the limit of large $k_{ff}/k_{off}$ values, all observed rate constants ($k_{in}$, $k_{out}$, and $k_{off}$) approach $k_{off}/2$ (*12*). For vesicles in which $k_{ff} > k_{off}$, the value for $k_{in}$ measured with pyranine would be much faster than that measured with ADIFAB, because pyranine quenching reflects dissociation of $H^+$ while ADIFAB which detects FFA directly would be limited by dissociation of FFA. Our measurements reveal virtually identical rate constants for pyranine and ADIFAB (Figures 6 and 7), thereby providing additional evidence that flip-flop is slower than dissociation. The simulations of Figure 2S also indicate that the measured rate constants $k_{in}$ and $k_{out}$ are similar to the model rate constants for vesicles in which flip-flop that is slower than dissociation.

## DISCUSSION

*Flip-Flop Is Slower Than Dissociation*. These results demonstrate that transport of FFA across lipid vesicle membranes is limited by the slow rate of flip-flop. These results agree well with those obtained in our previous studies (*12*, *13*) but are opposite those of Simard et al., who concluded that dissociation was rate-limiting and more than 9-fold slower than flip-flop (*14*). There are several reasons for this discrepancy. First, the evidence provided by Simard et al. (*14*), that flip-flop is significantly faster than dissociation, was the observation of identical rate constants for FFA dissociation and flip-flop when measured in vesicles containing both FPE and pyranine (Figure 2A,B of ref *14*). However, these vesicles, as we have now demonstrated, do not allow flip-flop to be distinguished from dissociation because the fluorescence of FPE obscures pyranine fluorescence (Figure 2). Therefore, such measurements do not provide information about flip-flop.

Second, Simard et al. (*14*) describe experiments (Figure 1 of ref *14*) suggesting that the time course of FFA influx, measured when using FFA−BSA complexes to deliver FFA to acceptor vesicles, reflects the rate of dissociation of FFA from BSA rather than FFA flip-flop. However, as the experiments illustrated in Figures 5 and 6 demonstrate, the rates of OA influx ($k_{in}$) are virtually identical when measured using OA−BSA complexes or OA-loaded donor vesicles to deliver OA to pyranine-containing acceptor vesicles. For both SUV and LUV, the rate constants for OA transferred from these vesicles ($k_{off}$) to acceptor SUV and LUV are significantly faster (for example, 3−10-fold at 25 °C) than the influx rate constants ($k_{in}$) (Tables 1 and 2). An additional indication that the flip-flop rate constants ($k_{in}$), measured with OA−BSA complexes, are independent of the rate of dissociation of OA from BSA, are the approximately 10-fold slower flip-flop rate constants obtained for LUV as compared to SUV, using the same OA−BSA complexes (Tables 1 and 2). The issue of whether dissociation from BSA is rate-limiting was also addressed by demonstrating that transfer of OA from OA−BSA complexes to ADIFAB is complete in less than 200 ms (*17*). In addition, kinetic model calculations reveal that transfer of FFA from BSA to vesicles is not rate-limited by the BSA dissociation rate constant (Figure 8 and ref *12*).

Third, Simard et al. (*14*) assert that FFA flip-flop should be determined by delivering FFA unbound rather than complexed with BSA, as reported previously by this group (*6*). However, as we demonstrated previously, influx measured using uncomplexed FFA yields rate constants that increase linearly with vesicle concentration (Figure 6 of ref *12*). Therefore, rate constants measured by such methods cannot be identified as flip-flop rate constants because flip-flop is unimolecular and must therefore be independent of vesicle concentration. In contrast, $k_{in}$ values measured by delivering FFA as complexes with BSA are independent of vesicle concentration (*12*, *13*). Moreover, we found that influx rate constants increased with increasing unbound OA concentration for $[OA_u] > 50$ nM (Figure 2 of ref *12*). This indicates that elevated unbound FFA perturb the vesicle bilayer. Accurately determining flip-flop rate constants ($k_{in}$) requires low $FFA_u$ (50 nM for $OA_u$) concentrations, and FFA−BSA complexes allow one to deliver such low concentrations reliably. In our influx measurements using donor vesicles to deliver OA, the donor vesicles were loaded with 2% OA, for which the $[OA_u]$ in equilibrium with the vesicles was 50 nM. Perturbation of the acceptor vesicles was observed when the donor vesicles were loaded with a larger mole percentage of OA (data not shown). The issue of a vesicle concentration dependence of $k_{in}$ was not addressed by Simard et al. (*14*).

*Rate Constants for Dissociation Are Faster Than Constants for Flip-Flop*. In this study, we measured dissociation of OA from SUV by two different methods: monitoring the transfer of OA between FPE-labeled and unlabeled SUV and the transfer of OA from donor SUV to BSA (Table 1). Results of both methods were equivalent, yielding an average value at 25 °C of 14.2 $s^{-1}$. This is in excellent agreement with the values of 13 ± 2 $s^{-1}$ at 22 °C and 14 $s^{-1}$ at 25 °C we obtained previously by monitoring transfer from SUV to BSA (*12*, *13*). Moreover, these results are virtually identical to the value of 13.5 $s^{-1}$ at 25 °C obtained by Massey et al. (*21*) from measurements of transfer of OA from SUV to anthraniloyl-labeled HSA (using a rate constant at 37 °C and an $E_a$ from Table 4 of ref *21*). In contrast, the value reported by Simard et al. (*14*) (7.2 ± 0.8 $s^{-1}$) is approximately half that obtained by ourselves and Massey et al. (*21*). Although we have no explanation for this discrepancy, even the value of 7.2 ± 0.8 $s^{-1}$ and certainly the consensus value of 13 $s^{-1}$ are faster than the flip-flop rate constant (5−6 $s^{-1}$) (Table 1). Similarly, LUV reveal faster OA dissociation than flip-flop in which LUV dissociation was monitored by the transfer from donor LUV to BSA (Table 2). The $k_{off}$ value of 6.2 $s^{-1}$ at 25 °C and our previous result of 5 $s^{-1}$ at 20 °C (*13*) are clearly faster than the flip-flop rate constants of 0.6 $s^{-1}$ from Table 2 and ref *13*. Dissociation that is faster than flip-flop is also demonstrated by the similar $k_{in}$ values found for pyranine- and ADIFAB-containing LUV (Figure 7 and Table 2) and for vesicles prepared by detergent dialysis (GUV) containing pyranine and ADIFAB (Figure 4 of ref *12*).

*Slow Flip-Flop Is Consistent with Proposed Mechanisms of Bilayer Permeability*. In a previous study, we investigated the FFA size and temperature dependence of transport of FFA through lipid vesicles (*13*). We found that the measured rate constants, $k_{in}$, $k_{out}$, and $k_{off}$, decreased exponentially with FFA size and that $k_{in}$ and $k_{out}$, but not $k_{off}$, were strongly temperature dependent. Earlier studies by Lieb and Stein revealed that the rate-limiting barrier to the permeability of solutes across red cell membranes decreased exponentially with the molecular volume of the solute (*22*). Lieb and Stein proposed that the rate of formation of a free volume large enough to accommodate a given solute was the rate-limiting barrier to the permeability of the nonelectrolyte solutes they investigated. This free volume model,

we suggested, was consistent with the exponential dependence on FFA size we observed, and because $k_{in}$ and $k_{out}$ were for all FFA less than $k_{off}$, we proposed that the barrier to FFA flip-flop across lipid vesicles was the rate of formation of a sufficiently large free volume. Moreover, we found, from the temperature dependence, that the activation free energy barrier to flip-flop, but not dissociation, was almost entirely enthalpic, suggesting that free volume formation involves specific chemical bonds. In contrast, the barrier to FFA dissociation was found to be largely entropic and was consistent with aqueous solvation of the FFA. These results provide a mechanistic basis for the slow FFA flip-flop that is the rate-limiting step for transport across the relatively simple lipid vesicle membranes of this study.

*Relationship of Transport of FFA across Lipid Vesicles to Transport across Cellular Membranes*. Characteristics of transport of FFA across lipid vesicles are significantly different than those of transport across cell membranes. Rates of transport across lipid vesicles are ~100 times faster than rates of cellular transport. For example, $k_{ff}$ for transport of oleate across LUV at 37 °C is ~2 $s^{-1}$ (Table 2 of ref *13*), while $k_{in}$ for adipocytes and preadipocytes is ~0.02 $s^{-1}$ (*23*). The initial rate of transport of FFA across cell membranes saturates with increasing extracellular [$FFA_u$] (*23*). For lipid vesicles, in contrast, $k_{in}$ increases with an increase in [$FFA_u$] (Figure 2 of ref *12*). Cellular transport is asymmetric with $k_{out}$ being approximately twice $k_{in}$ (*23*), whereas for lipid vesicles, $k_{in} \geq k_{out}$ (*13*). The saturable characteristics of cellular transport indicate that FFA are transported into the cells by a single pathway (*23*, *24*). FFA transported into the cells by this pathway are pumped up a concentration gradient, which is abolished by ATP depletion (*23*, *24*). These as well as other characteristics of cellular transport are not compatible with transport through a lipid bilayer phase of the plasma membrane and in fact are consistent with a lipid phase that is refractory to FFA transport. This suggests that the composition and/or structure of the lipid bilayer phase of cell membranes creates a barrier to flip-flop that is significantly larger than that in EPC vesicles.

## SUMMARY

In this study, we have shown that FPE and pyranine fluorescence cannot be resolved in vesicles containing both fluorophores, and therefore, the evidence for rapid flip-flop from such studies is invalid. We have also provided additional experimental as well as kinetic model evidence that FFA flip-flop is significantly slower than dissociation of FFA from lipid vesicles. Together with the results of our previous studies demonstrating that earlier evidence for rapid flip-flop was also invalid (*12*), we conclude that the rate-limiting step for transport of long chain FFA across lipid vesicles is flip-flop.

## ACKNOWLEDGMENT

We thank Rosita Moya-Castro for excellent technical assistance. We also thank J. Patrick Kampf and Laura Listenberger for help in preliminary studies and for useful discussions.

## SUPPORTING INFORMATION AVAILABLE

Results of measurements of dissociation of OA from SUV and vesicle to vesicle FFA transport time courses calculated using the kinetic model of eqs 1−4 are given. Rapid dissociation (15.7 $s^{-1}$) was revealed by monitoring transfer of OA from donor SUV to FPE-labeled acceptor SUV (Figure 1S). Kinetic model predictions for slow and rapid flip-flop reveal that the slow flip-flop predictions are consistent with our measurements (Figure 2SA). The calculations for rapid flip-flop reveal the surprising prediction that the rate constants for all compartments approach $k_{off}/2$ in the limit of very large $k_{ff}$ values and therefore that rapid flip-flop cannot be observed directly by the pyranine or ADIFAB methods (Figure 2SB,C). This material is available free of charge via the Internet at http://pubs.acs.org.

## REFERENCES

1. Kamp, F., and Hamilton, J. A. (2006) How fatty acids of different chain length enter and leave cells by free diffusion. *Prostaglandins, Leukotrienes Essent. Fatty Acids 75*, 149–159.
2. Kampf, J. P., and Kleinfeld, A. M. (2007) Is membrane transport of FFA mediated by lipid, protein, or both? Point/Counterpoint: An unknown protein mediates free fatty acid transport across the adipocyte plasma membrane. *Physiology 22*, 7–29.
3. Bonen, A., Chabowski, A., Luiken, J. J., and Glatz, J. F. (2007) Is membrane transport of FFA mediated by lipid, protein, or both? Mechanisms and regulation of protein-mediated cellular fatty acid uptake: Molecular, biochemical, and physiological evidence. *Physiology 22*, 15–29.
4. Daniels, C., Noy, N., and Zakim, D. (1985) Rates of Hydration of Fatty Acids Bound to Unilamellar Vesicles of Phosphatidylcholine or to Albumin. *Biochemistry 24*, 3286–3292.
5. Srivastava, A., Singh, S., and Krishnamoorthy, G. (1995) Rapid transport of protons across membranes by aliphatic amines and acids. *J. Phys. Chem. 99*, 11302–11305.
6. Kamp, F., Zakim, D., Zhang, F., Noy, N., and Hamilton, J. A. (1995) Fatty acid flip-flop in phospholipid bilayers is extremely fast. *Biochemistry 34*, 11928–11937.
7. Zhang, F., Kamp, F., and Hamilton, J. A. (1996) Dissociation of long and very long chain fatty acids from phospholipid bilayers. *Biochemistry 35*, 16055–16060.
8. Thomas, R. M., Baici, A., Werder, M., Schulthess, G., and Hauser, H. (2002) Kinetics and mechanism of long-chain fatty acid transport into phosphatidylcholine vesicles from various donor systems. *Biochemistry 41*, 1591–1601.
9. Storch, J., and Kleinfeld, A. M. (1986) Transfer of Long Chain Fluorescent Free Fatty Acids between Unilamellar Vesicles. *Biochemistry 25*, 1717–1726.
10. Kleinfeld, A. M., Chu, P., and Storch, J. (1997) Flip-flop is slow and rate limiting for the movement of long chain anthroyloxy fatty acids across lipid vesicles. *Biochemistry 36*, 5702–5711.
11. Kleinfeld, A. M., Chu, P., and Romero, C. (1997) Transport of long chain native fatty acids across lipid bilayer membranes indicates that transbilayer flip-flop is rate limiting. *Biochemistry 36*, 14146–14158.
12. Cupp, D., Kampf, J. P., and Kleinfeld, A. M. (2004) Fatty acid-albumin complexes and the determination of the transport of long chain free fatty acids across membranes. *Biochemistry 43*, 4473–4481.
13. Kampf, J. P., Cupp, D., and Kleinfeld, A. M. (2006) Different mechanisms of free fatty acid flip-flop and dissociation revealed by temperature and molecular species dependence of transport across lipid vesicles. *J. Biol. Chem. 281*, 21566–21574.
14. Simard, J. R., Pillai, B. K., and Hamilton, J. A. (2008) Fatty acid flip-flop in a model membrane is faster than desorption into the aqueous phase. *Biochemistry 47*, 9081–9089.
15. Richieri, G. V., Ogata, R. T., and Kleinfeld, A. M. (1992) A fluorescently labeled intestinal fatty acid binding protein: Interactions with fatty acids and its use in monitoring free fatty acids. *J. Biol. Chem. 267*, 23495–23501.
16. Richieri, G. V., Ogata, R. T., and Kleinfeld, A. M. (1999) The measurement of free fatty acid concentration with the fluorescent probe ADIFAB: A practical guide for the use of the ADIFAB probe. *Mol. Cell. Biochem. 192*, 87–94.
17. Kleinfeld, A. M., Storms, S., and Watts, M. (1998) Transport of long chain fatty acids across human erthrocyte ghost membranes. *Biochemistry 37*, 8011–8019.
18. Huber, A. H., Kampf, J. P., Kwan, T., Zhu, B., and Kleinfeld, A. M. (2006) Fatty acid-specific fluorescent probes and their use in resolving mixtures of different unbound free fatty acids in equilibrium with albumin. *Biochemistry 45*, 14263–14274.

19. Demant, E. J. F., Richieri, G. V., and Kleinfeld, A. M. (2002) Stopped-flow kinetic analysis of long-chain fatty acid dissociation from bovine serum albumin. *Biochem. J. 363*, 809–815.
20. Cullis, P. R., and Hope, M. J. (1991) Physical properties and functional roles of lipids in memranes. In Biochemistry of lipids, lipoproteins and membranes (Vance, D. E., and Vance, J., Eds.) 2nd ed., pp 1−40, Elsevier Science, Amsterdam.
21. Massey, J. B., Bick, D. H., and Pownall, H. J. (1997) Spontaneous transfer of monoacyl amphiphiles between lipid and protein surfaces. *Biophys. J. 72*, 1732–1743.
22. Lieb, W. R., and Stein, W. D. (1986) Non-Stokesian nature of transverse diffusion within human red cell membranes. *J. Membr. Biol. 92*, 111–119.
23. Kampf, J. P., Parmley, D., and Kleinfeld, A. M. (2007) Free fatty acid transport across adipocytes is mediated by an unknown membrane protein pump. *Am. J. Physiol. 293*, E1207–E1214.
24. Kampf, J. P., and Kleinfeld, A. M. (2004) Fatty acid transport in adipocytes monitored by imaging intracellular free fatty acid levels. *J. Biol. Chem. 279*, 35775–35780.